Persulfate activation by graphene oxide: practical and mechanistic insights concerning organic pollutants abatement

Alberto Cruz-Alcalde [a, *], Núria López-Vinent [a], Rui S. Ribeiro [b], Jaime Giménez [a], Carme Sans [a], Adrián M.T. Silva [b]

[a] *Department of Chemical Engineering and Analytical Chemistry, Faculty of Chemistry, Universitat de Barcelona, C/Martí i Franqués 1, 08028 Barcelona, Spain.*

[b] *Laboratory of Separation and Reaction Engineering - Laboratory of Catalysis and Materials (LSRE-LCM), Faculdade de Engenharia, Universidade do Porto, Rua Dr. Roberto Frías, 4200-465 Porto, Portugal.*

*Corresponding author: alberto.cruz@ub.edu

This article has been accepted for publication and undergone full peer review.
Please cite this article as DOI: 10.1016/j.cej.2021.130994

Abstract

Persulfate (PS) activation by means of graphene-based materials is a subject of increasing interest due to its potential as a water purification technology. Research efforts in this field have been mainly focused on tailoring the surface chemistry of graphene oxide (GO). However, the mechanism governing PS activation as well as some technological aspects should be considered in the design of the GO-PS system. In this work, the fundamentals and applicability of this process were addressed by catalytic oxidation experiments employing phenol as a model pollutant. Distilled, bottled and surface water, as well as a secondary-treated urban wastewater, were tested as matrices. The high performance of a commercial GO material (oxygen content: 4 wt.%) in PS activation was demonstrated through both batch and continuous mode experiments, using GO powders and membranes, respectively. In particular, continuous flow assays were conducted with the catalyst supported on a PTFE membrane for a total operation period of 7 d. Significant catalyst deactivation was gradually observed after 2-3 d, although recovery of the catalytic activity was possible through a simple thermal treatment of this material. Oxidation tests employing GO treated at different temperatures (500, 850 and 1000 ºC) were also performed and, together with the information drawn from the characterization results, it was possible to conclude that a shift in the character of the surface chemistry from acidic to basic enhances the catalytic activity of this material. Moreover, scavenging tests allowed inferring that singlet oxygen ($^1O_2$) is the oxidant species governing the degradation of the organic pollutant in this system. The mechanism responsible for the generation of this species seems to involve the nucleophilic attack of PS to C=O in basic pyrone-like functionalities.

Keywords: Water and wastewater treatment; graphene derivatives; surface chemistry; catalytic membranes; persulfate activation; singlet oxygen.

1. Introduction

Sulfate-based Advanced Oxidation Processes (AOPs) typically consist in the activation of persulfate (PS) or peroxymonosulfate (PMS) by means of agents such as ultraviolet light, heat, ultrasounds or catalysts, with subsequent yield of sulfate ($SO_4^{\bullet-}$) and hydroxyl ($HO^{\bullet}$) radicals [1,2]. The high reactivity and unselective character of these transient

species make these processes useful in the abatement of a wide variety of organic pollutants [1,3]. Catalytic materials may contain metals or not, although the latter are preferred since the metals used in this type of application may be rare, expensive or toxic, entailing sustainability issues [4,5]. Carbon materials, which are abundant and eco-friendly, represent some of the most promising solutions to avoid the use of metals in catalytic, sulfate-based AOPs. Particularly, graphene oxide (GO) derivatives are of special interest due to their relatively easy synthesis compared to other related materials and the potential for tailoring their surface chemistry in order to maximize the catalytic performance [5,6].

In the last decade, several works have reported the use of metal-free GO derivatives for PS or PMS activation and subsequent removal of organic pollutants from aqueous matrices. Most of these studies focused on the doping of GO with heteroatoms, mainly nitrogen alone [7–16] or in combination with others such as sulfur [17–19], boron or phosphorus [20]. The modification of these materials resulted in improved catalytic activities attributed to the presence of the heteroatoms and related chemical groups introduced by the doping procedure. However, PS and PMS can also be activated by non-doped GO: only a partial reduction in the oxygen content of the starting material appears to be required. Sun and coworkers reported the first evidences on the superior effectivity of a reduced GO in PMS activation when compared with other carbon materials [21]. After this first paper dealing with the use of a metal-free GO derivative to that purpose, subsequent publications confirmed its superiority also for PS activation [22–25]. Thus, reduced GO is considered a material of practical interest in terms of both PMS and PS activation, since simple thermal or hydrothermal reduction can be employed rather than complex heteroatom doping procedures.

In addition to the simplicity and cost of catalysts preparation, other practical aspects of the heterogeneous oxidation processes should be kept in mind when proposing a new water treatment solution, since all together dictate the technological, environmental and economic sustainability of potential real-world applications. It is well known that one of the main drawbacks of heterogeneous catalytic oxidation is the need of an additional step to separate the catalyst from water after treatment. In this sense, the use of catalytic membranes could be of advantage. To the best of the authors' knowledge, there are only four documents in the literature reporting the use of GO membranes for catalytic

activation of PS [26–29]. However, GO was doped with nitrogen in three of these previous works [26–28], and assembled with multi-walled carbon nanotubes in another study [29]. An additional critical aspect hampering the application of carbon materials as heterogeneous catalysts in oxidative treatments is the loss of catalyst activity. Catalyst deactivation and potential regeneration solutions have been barely addressed in the case of GO-based catalysts.

Moreover, the chemistry behind the observed activity in the GO-PS/PMS system is still under investigation, as some aspects related to the catalytic sites and produced oxidant species should be clarified. Regarding the first issue, it has been suggested that electron rich sp^2 carbon atoms located at the defective edges of the graphitic structure, as well as surface oxygen groups would be the principal activation sites for these oxidants [21,22,30,31]. Among different oxygen functionalities, the electron-rich ketonic/carbonyl group (C=O) appears to be the main reactive center based on experimental data and quantum chemical calculations [30,31]. At the same time, it has been observed that an excess in the oxygen content of the material is detrimental for the catalytic performance [21,22,31]. However, the optimal proportion of this atom and the contribution of the different oxygen functionalities on the PS/PMS activation performance have been seldom discussed. Concerning the oxidant species generated in the process, and although both radical (HO•, $SO_4^{\bullet-}$) and non-radical pathways appear to be possible, studies on reduced GO-PS/PMS oxidation mechanisms often report conflicting results. In some works, it is claimed that HO• is the main oxidizing species with some contribution by $SO_4^{\bullet-}$ [22]. In others, $SO_4^{\bullet-}$ is the dominant species and HO• contributes to a lower extent [23]. Finally, some documents state that a non-radical mechanism constitutes the prevailing pathway [25,32]. Some authors consider that the role of singlet oxygen ($^1O_2$) might be of importance in such cases [25]. Either way, it becomes clear that additional investigations are required to shed further light on these fundamental aspects.

Thus, the GO-PS system was comprehensively studied in this work with the aim of getting further insights on the underlying chemistry and applicability of this process in water treatment. A commercial GO material was employed to activate PS, which was selected over PMS because of its higher chemical stability and lower cost [2,33]. The activity and main influencing factors in the GO-PS process were first tested in batch oxidation experiments using phenol (Ph) as model organic contaminant, followed by longer

experiments in continuous mode with GO supported on PTFE membranes. Bottled water (BW), surface water (SW) and secondary-treated urban wastewater (WW) were used in addition to studies with distilled water. Tests in the presence of selected scavengers were also conducted to elucidate the main reactive species involved in this oxidation system. Moreover, GO treated at different temperatures were tested as catalysts, correlating the observed activity to the amount and type of oxygen functionalities on the materials surface.

2. Materials and methods

2.1. Chemicals and reagents

Phenol (Ph, 99%) and furfuryl alcohol (FA, 98%) were acquired from Sigma-Aldrich. Sodium persulfate (PS, 99%) was obtained from Riedel-de Häen. N,N-diethyl-p-phenylenediamine (DPD, 99%), sodium hydrogen phosphate (99%), sodium dihydrogen phosphate (99%) and sulfuric acid (95%), all of them required in PS analyses, were purchased from Fluka. Methanol (MeOH, 99.9%) was supplied by Fisher Scientific. Ultrapure water, which was used in Ph and PS analyses, was produced by a Direct-Q Millipore system. Unless otherwise specified, distilled water was employed in the rest of the work.

2.2. *Water matrices*

Four different water matrices were employed in the catalytic experiments: distilled water (DW) produced by a purification system; bottled water (BW, pH: 6.9; Dissolved Organic Carbon (DOC): not detected; Inorganic Carbon (IC): 1.8 mg L^{-1}; Cl^-: 5.6 mg L^{-1}) from the Portuguese commercial brand Fastio; surface water (SW, pH: 6.5; DOC: 1.8 mg L^{-1}; IC: 3.4 mg L^{-1}; Cl^-: 17.5 mg L^{-1}) collected from the Douro river in Porto (Portugal) and a treated wastewater (WW, pH: 7.0; DOC: 7.8 mg L^{-1}; IC: 34.8 mg L^{-1}; Cl^-: 56.1 mg L^{-1}) collected from the effluent of an urban WWTP located in Northern Portugal. The SW and WW samples were filtered through 0.45 μm cellulose filters and kept at 4 ºC until use.

2.3. Graphene-based materials

Graphene oxide (GO) was the material employed as catalyst in this work. It was acquired from Sigma-Aldrich. To investigate the mechanism of PS activation, three other materials were prepared by thermal treatment of GO under N_2 flow (100 mL min^{-1}) in a ThermoLab vertical oven, at different temperatures. In a first treatment step, which was common to all prepared materials, GO was treated at 120 ºC during 60 min. This temperature was reached through a heating ramp of 2 ºC min^{-1}. Then, a second treatment step was performed at different temperatures. A heating ramp of 2 ºC min^{-1} was set up to reach 500, 850 and 1000 ºC. These conditions were kept for 30 min. The materials prepared in this way were designated as rGO-500, rGO-850 and rGO-1000, with "rGO" standing for "reduced graphene oxide".

2.4. *Materials characterization*

Textural properties of GO and derived materials were determined from N_2 adsorption-desorption isotherms at -196 ºC, in particular the specific surface area (S_{BET}) as described in a previous publication [34]. Thermogravimetric analysis (TGA) was performed in a Netzsch STA 490 PC/4/H Luxx thermal analyser, in which the powder sample was heated in a gas flow from 50 to 1000 ºC at 10 ºC min^{-1}. Both inert (N_2) and oxidative (air) gas flows were employed.

Temperature programmed desorption (TPD) was performed in a fully automated AMI-300 Catalyst Characterization Instrument (Altamira Instruments), equipped with a quadrupole mass spectrometer (Dymaxion, Ametek), as described elsewhere [35]. The amount of CO_2 and CO were obtained by integrating the area of the respective spectra. Deconvolution analysis of the CO_2 and CO TPD spectra was performed using a well-established procedure [35,36]. Accordingly, the peaks in the CO_2 TPD spectra were assigned to different functional groups, namely: strongly acidic carboxylic acids (SA), less acidic carboxylic acids (LA), carboxylic anhydrides (CAn), and lactones (Lac). Likewise, the peaks in the CO TPD spectra were assigned to carboxylic anhydrides (CAn), phenols (Ph), carbonyls and quinones (CQ) and basic surface groups (Bas), such as pyrones and chromenes. In the CO_2 spectra, the width at half-height (W) was taken the same for CAn and Lac; in the CO spectra, the same W was considered for Ph and CQ whenever peak shoulders were unclear.

2.5. Catalytic oxidation experiments

Two different operation modes were used in GO-PS oxidation experiments: batch and continuous flow. In batch experiments, 5 mg L^{-1} or 30 mg L^{-1} phenol solutions containing 0.25-1 mM of PS were prepared and placed in 8 mL amber glass bottles equipped with a stirring bar, which were employed as reactors. In some of these tests, *tert*-butanol (tBuOH), methanol (MeOH) or furfuryl alcohol (FFA) were also added in excess (100 mM) to act as scavengers for oxidant species. In general, experiments started with the addition under vigorous stirring of GO (or derived materials) powder at varying dosages (0.25-1 g L^{-1}). Samples were withdrawn at regular time intervals and filtered through 0.2 µm PTFE syringe filters. All batch catalytic assays were conducted for 90 min. In continuous flow experiments, GO membranes (effective area: 2.1 cm^2) were tested in dead-end mode. These were prepared by vacuum filtration of aqueous GO dispersions (0.2-0.5 g L^{-1}) through 0.2 µm Omnipore PTFE membranes, resulting this in a supported amount of catalyst of 5-15 mg. Aqueous solutions of Ph (5 mg L^{-1}) containing 1 mM of PS were placed in a stirred reservoir and continuously fed to a glass membrane cell at a flow-rate of 0.1-0.5 mL min^{-1}, by means of an Ismatec 829 peristaltic pump (Cole-Parmer, USA). A detailed scheme of the setup employed in continuous mode experiments can be found elsewhere [28]. Samples were collected from the filtrate at regular time intervals. In this case, experiments were conducted for at least 24 h and up to 7 d. Regardless of the operation mode, all catalytic experiments were performed at room temperature (25 ºC) and the natural pH conditions of the water matrix (pH 7 in the case of experiments conducted with distilled water). Control experiments without the addition of PS were performed to evaluate the adsorption of Ph onto GO and derived materials. The stability of Ph in PS solutions (i.e., without the presence of GO) was also tested. In all cases, samples were frozen after withdrawal and kept at these conditions until approximately 1 h before analysis.

2.6. Analytical techniques

Phenol concentration was determined by means of an Elite LaChrom HPLC equipped with an L-2450 Diode Array Detector (DAD), all supplied by Hitachi. The employed column was a Lichrocart Purospher Star RP-18 endcapped column (250 mm x 4.6 mm, particle size of 5 µm). The mobile phase consisted of 70:30 volumetric mixtures of water

and methanol. The flowrate and injection volume were set, respectively, at 0.5 mL min^{-1} and 50 µL. Detection was performed at 270 nm. The concentration of persulfate was determined by the N,N-diethyl-p-phenylenediamine (DPD) colorimetric method [28]. Dissolved Organic Carbon (DOC) content was determined with a Shimadzu TOC-L analyzer.

3. Results and discussion

3.1. Materials characterization

GO is a commercial multilayer material with 15-20 stacked graphene sheets (as described by the supplier) and a low ash content (TGA residue of *ca.* 1 wt.%; determined under oxidative atmosphere, as shown in Fig. S1a). Both the pristine GO and derivatives of this material obtained by thermal treatment at different temperatures and employed later on in this work for the mechanistic study of the process (Section 3.3.1), were characterized. The N_2 adsorption-desorption isotherms are given in Fig. S2, and the respective S_{BET} values are summarized in Table 1. As observed, all the materials have S_{BET} values in the range 262-281 m^2 g^{-1}. Therefore, it can be concluded that the textural properties of the resulting materials are negligibly affected upon thermal treatment of GO, regardless of the temperature employed. This is of utmost importance for this study, since maintaining textural properties unaltered is crucial to elucidating the influence of surface chemistry in the catalytic properties.

The effect of the different thermal treatments on the surface chemistry properties of the graphene-based materials was investigated by TGA and TPD. The former allows determining the total volatile content, while the latter allows quantifying and identifying different oxygen containing surface groups, which are released as CO_2 and CO upon heating [35,36]. The CO_2 and CO TPD spectra of the graphene-based materials are given in Figs. 1a and b, respectively. The total amount of surface groups released as CO_2 and CO (determined from the area under the TPD spectrum) and the corresponding oxygen content (calculated from the total amounts of CO_2 and CO released from the surface of the carbon materials), are summarized in Table 1.

Table 1. Specific surface area (S_{BET}), amount of volatiles (determined by TGA), amounts of CO_2 and CO released by TPD, and corresponding percentage of oxygen (assuming that all the surface oxygen is released as CO_2 and/or CO).

Material	S_{BET} ($m^2\ g^{-1}$)	Volatiles (wt.%)	[CO_2] ($\mu mol\ g^{-1}$)	[CO] ($\mu mol\ g^{-1}$)	O (wt.%)	CO/CO_2
GO	266	14.9	1044	408	4.0	0.4
rGO-500	262	13.3	395	821	2.6	2.1
rGO-850	276	5.6	0	360	0.6	n.a.
rGO-1000	281	4.7	0	239	0.4	n.a.
$GO_{Continuous}$	n.d.	n.d.	1508	979	6.4	0.6
GO_{Batch}	n.d.	15.2	824	1022	4.3	1.2
$GO_{Regenerated}$	n.d.	9.3	217	970	2.3	4.5

n.a.: not applicable; n.d.: not determined.

Graphene oxide is defined as a monolayer material, characterized by C/O atomic ratios less than 3 and typically close to 2 [37]. Therefore, the first conclusion to be withdrawn from the results given in Table 1 is that the commercial GO employed in this study can actually be described as a partially reduced GO, considering both its multilayer configuration (as mentioned above) and the relatively low surface oxygen content (4.0 wt.%, as determined by TPD). Notwithstanding, the amount of oxygen containing surface groups decreases as the temperature of the thermal treatment increases. This trend becomes particularly clear when the oxygen content of the graphene-based materials is plotted against the temperature of the thermal treatment (Fig. 2a), a near linear correlation being obtained. This evolution is followed by the decrease of volatiles (Table 1). An illustrative example of the TGA performed for the determination of the volatile content of the materials is shown in Fig. S1b.

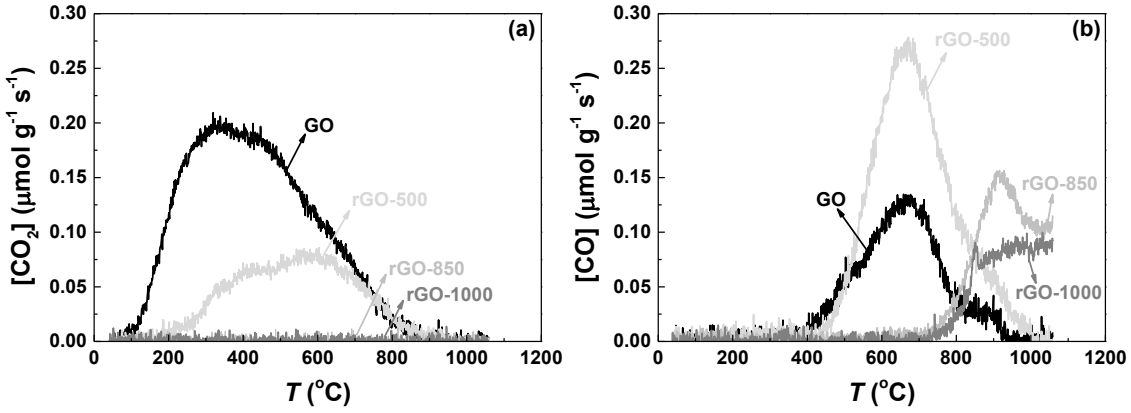

Figure 1. TPD spectra of the graphene-based materials: (a) CO_2 and (b) CO evolution with temperature.

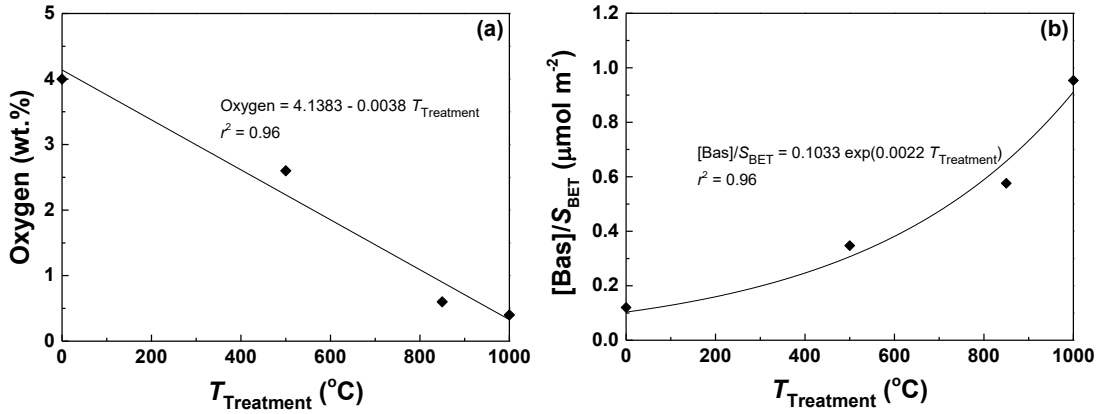

Figure 2. (a) Oxygen content and (b) [Bas]/S_{BET} as a function of the temperature employed in the thermal treatment ($T_{Treatment}$) of GO. Points represent experimental data, while lines represent (a) linear and (b) exponential fittings.

Deconvolution analysis of the CO_2 and CO TPD spectra was performed as described in Section 2.4, in order to identify and quantify the functional groups originally present at the surface of GO, as well as those removed and/or generated during the thermal treatments under the inert atmosphere of N_2. The deconvolution spectra are given in Fig. 3 for the pristine sample and Fig. S3 for the thermally treated GO samples, the corresponding results being detailed in Tables S1 and S2, respectively. From these results, it can be concluded that the decrease of oxygen containing groups previously commented is due to the selective removal of functionalities whose decomposition temperature is below that employed in the thermal treatment. For instance, all the strongly acidic carboxylic acids (SA), originally released at around 248 ºC in the pristine GO (Fig. 3a and Table S1), are removed upon thermal treatment at 500 ºC during 30 min (Fig. S3a). However a fraction of less acidic carboxylic acids (LA), originally released at around 400 ºC, subsists after the thermal treatment. This phenomenon has already been reported in a study in which carboxylic acids were still detected by X-ray photoelectron spectroscopy (XPS) after thermal treatment of rGO at 400 ºC during 60 min []. Nevertheless, the results suggest that some of these less thermally stable groups are in fact converted into others with higher thermal resistance, such as those containing highly stable carbonyl and ether groups. These chemical changes of oxygen-containing functional groups have been elucidated elsewhere [], and are particularly evident in the case of basic surface groups (Bas), such as pyrones and chromenes, which decompose at the highest temperatures. Indeed, the amount of these functionalities increases almost exponentially as the

temperature of the thermal treatment increases, as revealed when the concentration of Bas determined by TPD is normalized by the S_{BET} of the graphene-based materials (i.e., ([Bas]/S_{BET}), and represented as a function of the temperature employed in the thermal treatment (Fig. 2b). It is noteworthy that carbonyls and quinones (CQ) are still detected by TPD after thermal treatment at both 850 ºC and 1000 ºC (Fig. S3a and Table S2). This is in agreement with a previous study revealing thermal resistance of these groups up to around 1230 ºC when embedded to graphene-based materials [].

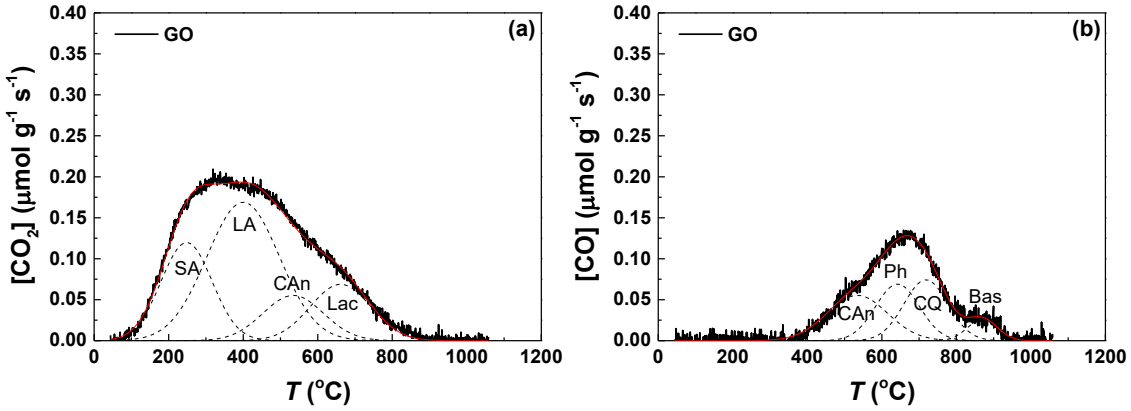

Figure 3. Deconvolution results of (a) CO_2 and (b) CO TPD spectra of GO. Dashed lines represent peaks assigned to strongly acidic carboxylic acids (SA), less acidic carboxylic acids (LA), carboxylic anhydrides (CAn), lactones (Lac), phenols (Ph), carbonyls and quinones (CQ) and basic surface groups (Bas), such as pyrones and chromenes. Red lines represent cumulative peak fitting.

3.2. Performance of PS activation by GO

3.2.1. Batch mode experiments

Batch catalytic experiments were first performed to test the activity of commercial GO in PS activation for the removal of phenol at 5 mg L^{-1}, under different catalyst and oxidant dosages. Results are presented in Fig. 4. Adsorption tests (Fig. 4a) and controls without addition of GO were also performed to test the individual contribution of both catalyst and oxidant, respectively, to the overall removal of Ph. No abatement of Ph by the only action of PS was observed in 90 min (data not shown). Concerning adsorption experiments, these revealed that the Ph removals increased with the doses of GO, maximum adsorption levels in the range between 20 and 70% of the initial Ph content being obtained (i.e. for the lowest and highest GO content tested, respectively). Catalytic

oxidation experiments (Figs. 4b and c) showed that a great improvement in the removal process can be achieved upon addition of PS. This makes clear that GO is an excellent activator for PS, and confirms the observations made in previous related studies [22,23]. For instance, in experiments employing GO doses of 0.5 g L^{-1}, all the initial Ph was removed in only 10 min. The contribution of adsorption mechanisms together with the excellent activating properties of GO might be responsible for the results obtained in these tests. It is also worth to mention that additional catalytic experiments conducted with complex water matrices (i.e., BW, SW and WW) also revealed excellent Ph removal performances (Fig. 4d). Only in the case of the assay conducted with the wastewater, a significant decrease in the abatement rate was observed. This can be attributed to the higher content of background inorganic and organic carbon species competing for the oxidants produced in the GO-PS system (Section 2.2).

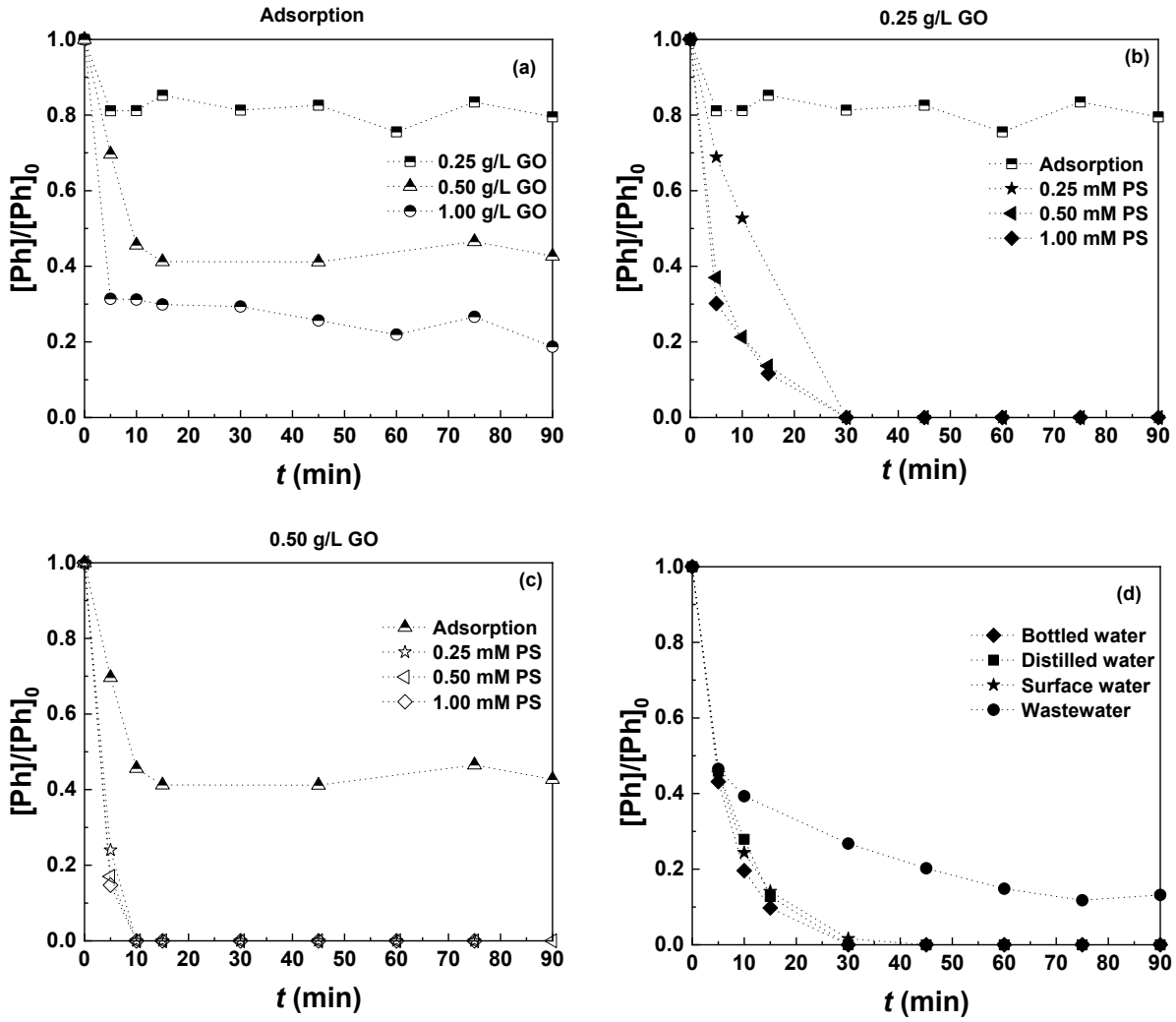

Figure 4. Influence of catalyst (commercial graphene oxide, GO) and oxidant (persulfate, PS) dose for phenol abatement in distilled water and performance of the process in actual water matrices. a) Adsorption tests; b) Oxidation tests with 0.25 g L^{-1} GO; c) Oxidation tests with 0.50 g L^{-1} GO; d) Experiments in actual water matrices with 0.25 g L^{-1} GO and 0.25 mM PS. $[Ph]_0$ = 5 mg L^{-1} in all cases.

3.2.2. *Continuous mode experiments*

GO membranes were prepared and tested in continuous operation mode for PS activation in the removal of phenol at 5 mg L^{-1}. The PS dose was kept at 1 mM in all cases, studying the process performance at different flow-rates (0.1, 0.25 and 0.5 mL min^{-1}, 15 mg of catalyst in all cases) and amounts of supported GO (1, 5 and 15 mg, 0.1 mL min^{-1} in all cases). Results for a total operation time of 24 h are shown in Fig. 5a and Fig. S4. The lower flow-rate value tested (i.e., 0.1 mL min^{-1}) resulted in better activation efficiencies and therefore a higher and more sustained removal of Ph, probably because of a better

contact between GO and PS achieved at lower flow velocities (Fig. S4b). In the case of experiments with 1 and 5 mg of supported GO, a transient state was firstly observed during the first hours of operation until the maximum oxidation efficiency was reached, followed by a gradual decrease of the process performance for the remaining of the experimental period. This progressive decrease in the observed activity was less pronounced in the case of membranes containing the highest load (i.e., 15 mg) of catalyst (Fig. S4a). In this case, in fact, an almost steady removal of Ph of about 90% was observed in the period between 2 and 24 hours. Thus, higher maximum removals of Ph were observed for membranes containing larger amounts of catalyst, as already observed in previous experiments using catalytic membranes prepared with N-doped GO [26].

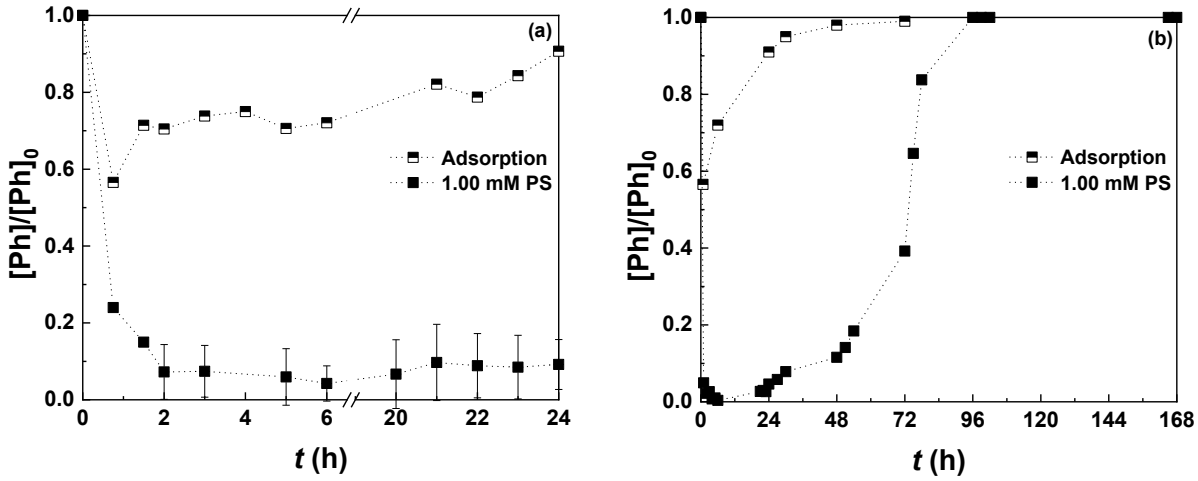

Figure 5. Oxidation and adsorption experiments for phenol degradation using PTFE-supported GO membranes tested in continuous mode, in distilled water. a) 24 h-test; b) 168 h-test. $[Ph]_0$ = 5 mg L^{-1}, $[GO]_0$ = 15 mg; $[PS]_0$ = 1 mM; flow-rate = 0.1 mL min^{-1}.

The catalytic stability of the GO membrane was further tested through continuous operation experiments performed for a period of 1 week. A catalyst load of 15 mg and a flow-rate of 0.1 mL min^{-1} were applied in this case, as these were the best performing conditions according to the previous screening of influential factors. Simultaneously, a separate control experiment without the presence of PS was also conducted for the same period of time. Results are presented in Fig. 5b. Relatively high removal levels of Ph were initially observed in the adsorption control test (as high as 40%), followed by a period characterized by a gradual decrease in the Ph removal efficiency through this mechanism. A steady $[Ph]/[Ph]_0$ value of 1 was observed after 3 days of operation, indicating that the

saturation of the material was reached. Regarding the catalytic test, very high removals (i.e., > 90%) of the model compound were registered during the first 48 h, although a slow but gradual decrease in the oxidation efficiency was also observed. The period from 48 to 72 h was characterized by a significant loss of the catalytic activity (from 90 to 60% Ph removal), followed by a dramatic drop in the next 24 h (from 60 to 0% removal). The evolution of PS in this experiment, represented in Fig. S5, is in agreement with the observed phenol abatement throughout the same operation period. From a time of approximately 96 h, and until the end of the operation period, consumption of this oxidant source was not observed.

3.2.3. *Catalyst deactivation and regeneration*

To shed some light on the causes behind the observed loss in the catalytic activity, GO recovered from the membrane employed during 1 week (designated as $GO_{Continuous}$) was characterized by TPD. The corresponding CO and CO_2 spectra, together with those of pristine GO, are shown in Fig. 6. The amount of oxygen-containing groups on GO surface significantly rose during the operation period, leading to an overall 60% increase in the oxygen content compared to the starting material (Table 1). This value is close to the ca. 80% increase reported by Duan et al. in previous studies regarding catalyst stability in the GO-PS and GO-PMS systems [22,32]. A deeper look via TPD spectra deconvolution (Figs. S6a and b for spectra deconvolution and Tables S1 and S2 for detailed results) revealed that phenols, carboxylic anhydrides and less acidic carboxylic acids, with the amount increasing 400, 100 and 75%, respectively, constituted the oxygen-containing groups whose amount on GO surface rose in a more significant way. These changes are explained by the adsorption of the model pollutant (i.e., phenol) and transformation products (TPs) on the catalyst surface, which probably hindered the adsorption-activation of PS molecules [21–23]. A fraction of the new LA and CAn moieties, suspected of being poorly active sites [30], might alternatively have resulted from the oxidation of other oxygen functionalities contained in the pristine GO, such as CQ (45% decrease) or Ph [30,32].

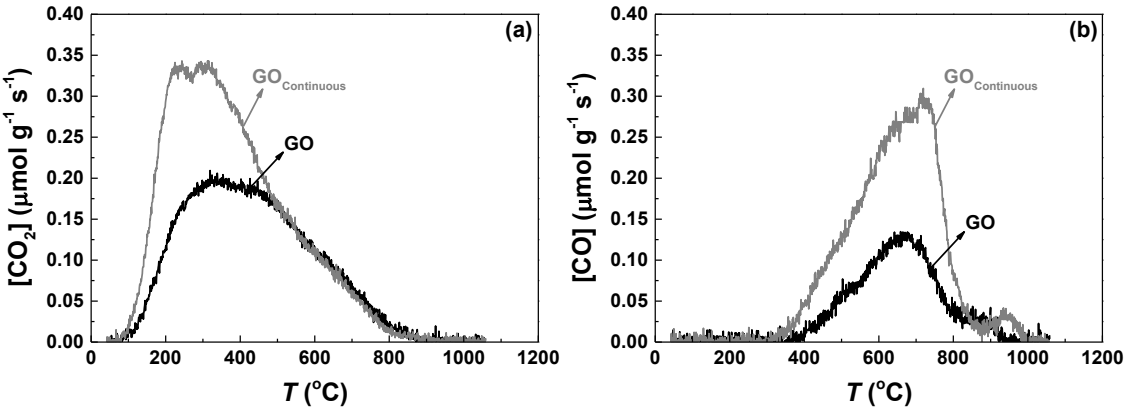

Figure 6. TPD spectra of GO prior and after the experiment performed in continuous mode during 1 week ($GO_{Continuous}$): (a) CO_2 and (b) CO evolution with temperature.

A simple strategy to regenerate the deactivated catalyst may be based on thermal desorption of substances causing saturation. To test this approach, the catalyst used in a batch experiment (GO_{Batch}) was recovered and thermally treated at 500 ºC under N_2 flow ($GO_{Regenerated}$). Then, this material was employed as a catalyst in an additional batch oxidation test. A similarity in the Ph degradation profiles was observed in experiments with GO and $GO_{Regenerated}$ (Fig. 7), indicating that the catalytic activity of the starting material can be successfully recovered through this procedure. This is in line with the findings of two previous works by Duan and coworkers, although the temperatures used for material regeneration in these studies were 350 and 400 ºC, resulting only in partial recoveries of the catalytic activity [22,32].

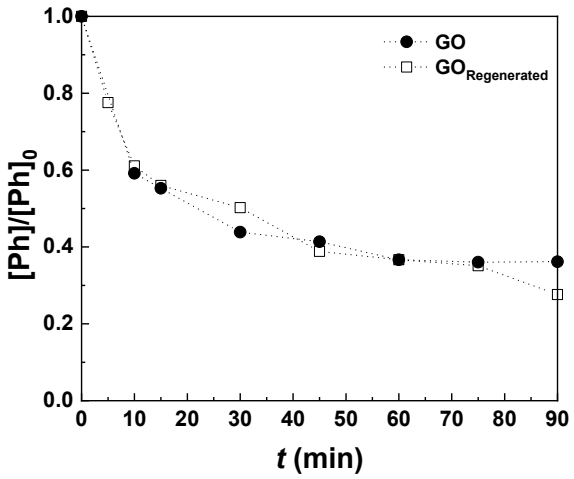

Figure 7. Catalytic oxidation of Phenol in GO-PS experiments with pristine and thermally regenerated GO. $[Ph]_0 = 30$ mg L^{-1}, $[GO]_0 = 0.25$ mg L^{-1}, $[PS]_0 = 1$ mM.

Based on TPD data (Tables 2, S1 and S2, as well as Figs. S6c-f), the oxygen content in GO_{Batch} was only slightly higher than that of GO, even though very significant differences were observed in the amount of some oxygen groups such as Ph, LA or SA. The great increase in the Ph moieties amount (by 444%) can be ascribed to adsorption of the model pollutant and phenolic TPs, as already observed in the case of $GO_{Continuous}$. Contrarily to what was found in that case, a significant reduction in the concentration of LA groups (68% decrease) compared to GO was observed in GO_{Batch}, whereas the SA amount increased by 41%. A simple explanation to these apparently discrepant results can be related to operational differences in batch and continuous mode experiments, including the solid-liquid contacting system, the PS concentration and the GO operation time. Since adsorption and oxidation kinetics in these systems are mostly operationally defined, different experimental conditions might have resulted in distinct process efficiencies, this leading to different final distributions of TPs and oxygen functionalities on the surface of the catalyst. On its part, $GO_{Regenerated}$ displayed a lack of SA and LA surface groups due to the temperature employed in the regeneration procedure, and a general reduction in CAn, Lac and Ph groups compared to GO_{Batch}, which was also attributed to the effect of heat energy. On the other hand, CQ and Bas increased their relative amount by 78 and 228%, respectively, compared to the same material. As observed in Section 3.1 for materials treated at different temperatures, transformations from less to more thermally resistant surface oxygen groups are apparently possible. Overall, changes produced in the surface chemistry during material regeneration resulted in a decrease in the oxygen content of about 45% compared to both GO_{Batch} and GO.

According to the above results, it can be inferred that the catalytic activity displayed by $GO_{Regenerated}$ is very similar to that observed with pristine GO, which can be ascribed to a partial or even total removal of slight to moderately acidic compounds previously adsorbed (i.e., phenol and its corresponding TPs). Changes in the character of GO oxygen groups to less acidic functionalities might also have an influence on the catalytic performance, although both the relative importance of this deactivation mechanism and in general the contribution of oxygen groups on GO catalytic activity require further study.

3.3. *Mechanism of PS activation by GO*

With the aim of understanding the mechanism behind the GO-PS oxidation system, two additional investigations were conducted. In first place, batch catalytic experiments were carried out with thermally modified GO in order to discern which surface oxygen groups are involved in PS activation. Then, scavenging tests were conducted to get further insights on the nature of the reactive species formed upon activation and subsequently acting as oxidants. An activation mechanism of PS by GO was then proposed based on the observed results and current related knowledge.

3.3.1. Role of O-containing functionalities on activation mechanism

GO derivatives prepared by thermal treatment at different temperatures (*i.e.*, rGO-500, rGO-850 and rGO-1000) were tested as catalysts in additional batch experiments. The resulting Ph abatement curves are shown in Fig. 8a. As observed, the degradation of phenol was faster when employing GO derivatives prepared with increasing treatment temperatures. Considering the negative correlation between surface oxygen content and treatment temperature (Fig. 2a), these results confirm the inverse trend between catalytic activity and the oxygen percentage already suggested by the data obtained in previous studies on PS and PMS activation by GO [21,22,31,32].

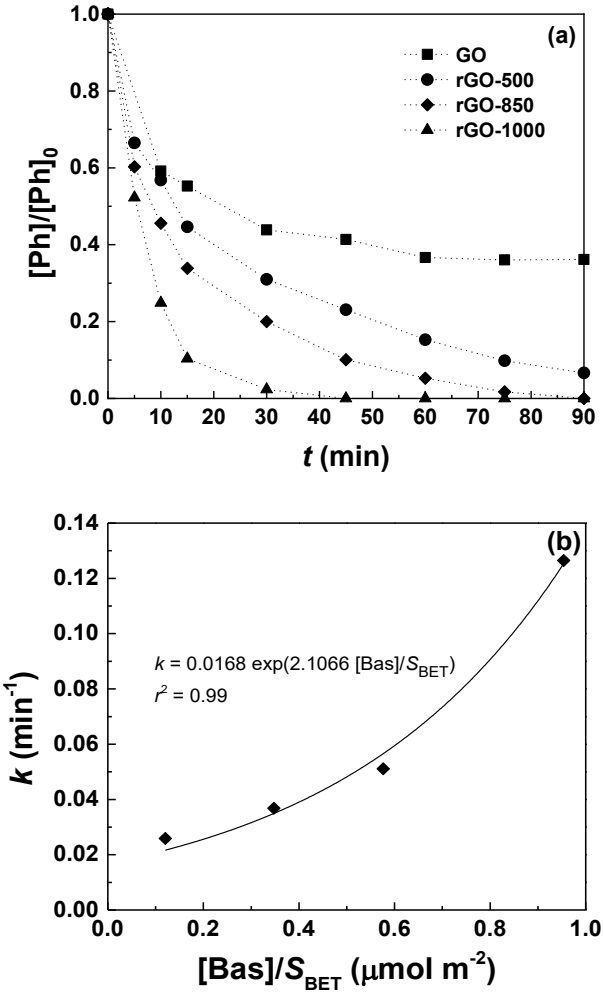

Figure 8. Catalytic oxidation of phenol in GO-PS experiments with pristine and thermally treated GO at different temperatures. a) Degradation profiles; b) Dependence of pseudo first order rate constant for Ph degradation with the S_{BET}-normalized concentration of oxygen basic surface groups ([Bas]/S_{BET}). $[Ph]_0$ = 30 mg L^{-1}, $[GO]_0$ = 0.25 mg L^{-1}, $[PS]_0$ = 1 mM.

As discussed, reduction of the overall surface oxygen content in GO upon thermal treatment at increasing temperatures is accompanied by a progressive shift in the type of functionalities, from acidic to basic (Tables S1 and S2). Accordingly, the fact that decreasing the oxygen contents to very low percent values results in a significant improvement of the catalytic activity might be explained by two different phenomena, though partly related and in fact simultaneous. On one hand, acidic O functionalities, like SA and LA, may hinder PS activation by causing an electron-withdrawing effect at GO reactive centers. At the same time, a rise in the concentration of more basic, and electron donor, oxygen groups such as CQ and Bas would increase the possibility of electron-transfer or nucleophilic reactions with PS, resulting in a faster activation of this molecule

and subsequent oxidation of the model compound. The positive influence of basic groups becomes particularly evident when plotting the pseudo first order rate constant of phenol degradation against [Bas]/S_{BET} (Fig. 8b). The observed exponential correlation suggests a strong dependence of GO activity with the concentration of the most basic surface oxygen functionalities. Some of these, such as pyrone moieties, contain carbonyl functions (C=O) which are thought to be important catalytic sites amongst oxygen functionalities on GO surface [30,31]. The fact that rGO-1000 performed better as a catalyst than rGO-850 constitutes an additional evidence of this. As seen in Tables S1 and S2, only CQ and Bas surface functions were present, being the concentration of Bas groups 41% higher in the case of rGO-1000. The amount of CQ groups, on its part, was reduced by 77% from rGO-850 to rGO-1000.

The results obtained in this work constitute additional insights on the nature of GO catalytic sites and support the role of carbonyl groups in PS activation. In addition, the basicity of the reactive centers appears to play a key role in the process and may trigger the study of other basic oxygen functions different from those containing ketone moieties (e.g., chromenes) as potential reactive centers. Furthermore, these results point out the possibilities of a simple yet powerful method (i.e., thermal treatment) for potential tuning of the GO surface chemistry.

3.3.2. Scavenging tests and evidences of non-catalytic oxidation mechanism

According to the previous literature, it can be assumed that the strong oxidants potentially generated in the GO-PS process may be HO•, $SO_4^{\bullet -}$ and $^1O_2$. Their relative contributions to organic pollutants oxidation can be elucidated if a selective removal of these species from the reaction medium is achieved. The study of the oxidants responsible for pollutants degradation in the GO-PS system was therefore conducted by means of batch catalytic experiments with addition of different scavengers, namely *tert*-butanol (tBuOH), methanol (MeOH) and furfuryl alcohol (FFA). Results are presented in Fig. 9.

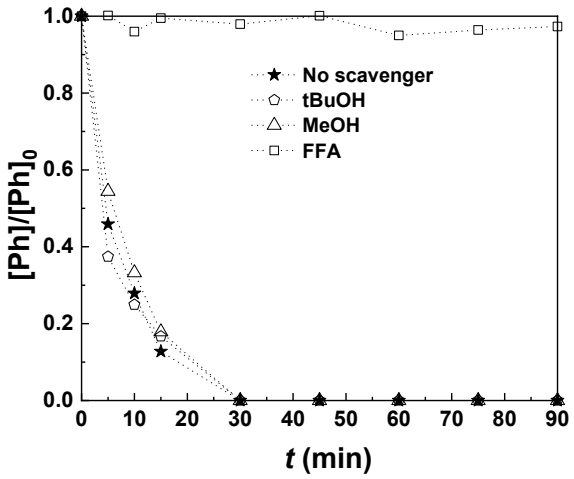

Figure 9. Catalytic oxidation of Ph via GO-PS process in the presence of various scavengers. $[Ph]_0$ = 5 mg L^{-1}, $[GO]_0$ = 0.25 mg L^{-1}, $[PS]_0$ = 0.25 mM, $[tBuOH]_0 = [MeOH]_0 = [FFA]_0$ = 100 mM.

Ph degradation profiles observed in experiments with tBuOH and MeOH addition were almost identical to that obtained in the assay performed in the absence of scavengers. The only exception was found in the experiment conducted with FFA, for which the abatement of the model compound was completely inhibited. tBuOH reacts fast with HO• ($k_{tBuOH, HO•}$ = $6 \cdot 10^8$ M^{-1} s^{-1} [38]), whereas it presents markedly slower kinetics with $SO_4^{\bullet-}$ ($k_{tBuOH,SO4•-}$ = $9 \cdot 10^5$ M^{-1} s^{-1} [39]). On its part, $SO_4^{\bullet-}$ was suppressed by adding MeOH ($k_{MeOH,SO4•-}$= $2 \cdot 10^7$ M^{-1} s^{-1} [39]), which also reacts fast with HO• ($k_{MeOH, HO•}$ = $9.7 \cdot 10^8$ M^{-1} s^{-1} [38]). Moreover, $^1O_2$ reactions with tBuOH and MeOH are slow ([40], rate constant value not available). Finally, FFA undergo fast reaction with $^1O_2$ ($k_{FFA,1O2}$ = $1.2 \cdot 10^8$ M^{-1} s^{-1} [40]), although this alcohol also presents a high reactivity towards HO• ($k_{FFA, HO•}$ = $1.5 \cdot 10^{10}$ M^{-1} s^{-1} [38]) and most probably also with $SO_4^{\bullet-}$ (kinetic data not found). According to this analysis and the results obtained, singlet oxygen arises as the dominant (if not the only one) oxidant in the GO-PS system. This is in contrast with conclusions drawn in some previous studies concerning the same process, in which organic compounds oxidation has been primarily attributed to $SO_4^{\bullet-}$ [23] or HO• [22]. However, in addition to potential differences in the composition of the employed catalysts, none of the previous works assessed the potential contribution of non-radical oxidants (e.g., $^1O_2$) in the overall degradation process, underestimating the role of the non-radical pathway.

A pathway for $^1O_2$ formation was finally proposed based on the results obtained in the scavenging tests, the insights on the role of surface oxygen groups revealed in the former

section and mechanistic considerations from previous literature. In addition, involvement of dissolved oxygen in $^1O_2$ formation was discarded in batch experiments under N_2 bubbling (Fig. S7). The mechanism is depicted in Fig. 10 considering some of the most basic pyrone-like model moieties [41]. PS activation by GO could thus proceed via nucleophilic addition of this molecule to the carbonyl group of pyrone-like functions (reaction I), resulting in the formation of a dioxirane intermediate (reactions II and III). This species would then undergo nucleophilic attack by another persulfate molecule to yield $^1O_2$ and recover the initial ketone group (reaction IV). The suggested mechanism is analogous to that described for $^1O_2$ production through PMS reaction with ketone groups in benzoquinone [42]. In this case, though, the symmetrical charge distribution of the peroxide bond in PS makes this reaction less probable compared to PMS (which has an asymmetrical O-O bond), although still possible. This pathway has in fact been also proposed to explain singlet oxygen production via PS activation by carbon nanotubes [43].

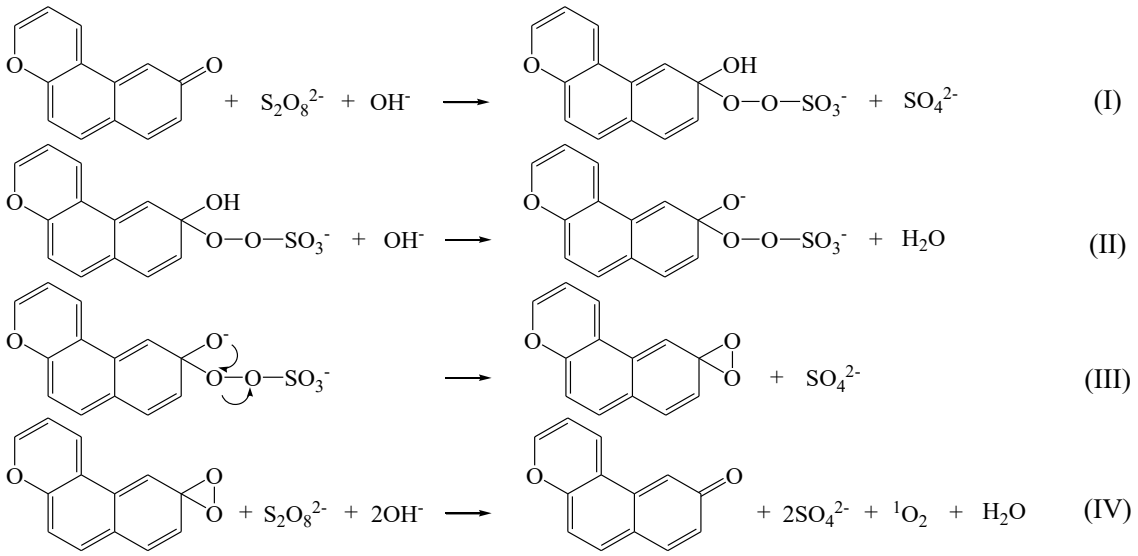

Figure 10. Proposed mechanisms for $^1O_2$ production upon PS activation on GO basic surface oxygen groups, described for a pyrone-like model moiety.

Conclusions

The use of GO as catalyst for PS activation can be of advantage in applications aiming at the abatement of organic compounds from aqueous matrices. The per se high catalytic performance of commercially available materials with low oxygen contents (e.g. 4 wt.%) may be further improved by applying a simple thermal treatment. This rise in GO activity

693 is ascribed to a shift in the predominant surface oxygen groups from acidic to basic, which
694 is gradually achieved with increasing treatment temperatures. The presence of basic
695 functionalities appears to be particularly relevant for continuous production of $^1O_2$ upon
696 PS nucleophilic attack on C=O moieties. Regarding the viability of the process as a water
697 treatment technology, the immobilization of GO on a polymeric membrane arises as a
698 promising approach to solve one of the most common shortcomings of heterogeneous
699 oxidation processes (i.e., the need of an additional step to separate the catalyst from the
700 treated water). Catalyst deactivation issues, on their part, may be mitigated by a simple
701 thermal regeneration procedure. Further research is encouraged concerning mechanistic
702 aspects (e.g., reactions involving pyrone and chromene-like functionalities), the
703 optimization of membrane design and operating conditions and the testing of this process
704 in more realistic scenarios, including assays in water and wastewater matrices of different
705 quality and considering the abatement of a broader range of organic pollutants at trace
706 concentrations.
707
708 **Acknowledgements**
709
710 This work was financially supported by project NORTE-01-0145-FEDER-031049
711 (InSpeCt - PTDC/EAM-AMB/31049/2017) funded by FEDER funds through NORTE
712 2020 - Programa Operacional Regional do NORTE, and by national funds (PIDDAC)
713 through FCT/MCTES. We would also like to thank the scientific collaboration under
714 Base Funding - UIDP/50020/2020 of the Associate Laboratory LSRE-LCM - funded by
715 national funds through FCT/MCTES (PIDDAC). AC and NL are grateful to the Spanish
716 Government for their postdoctoral (BES-2015-074109, POP stage) and PhD (FPU-
717 16/02101) fellowships, respectively.
718
719 **References**
720
721 [1] J. Wang, S. Wang, Activation of persulfate (PS) and peroxymonosulfate (PMS)
722 and application for the degradation of emerging contaminants, Chem. Eng. J. 334
723 (2018) 1502–1517. https://doi.org/10.1016/j.cej.2017.11.059.
724 [2] S. Wacławek, H. V. Lutze, K. Grübel, V.V.T. Padil, M. Černík, D.D. Dionysiou,
725 Chemistry of persulfates in water and wastewater treatment: A review, Chem. Eng.
726 J. 330 (2017) 44–62. https://doi.org/10.1016/j.cej.2017.07.132.

[3] U. von Gunten, Oxidation Processes in Water Treatment: Are We on Track?, Environ. Sci. Technol. 52 (2018) 5062–5075. https://doi.org/10.1021/acs.est.8b00586.

[4] D.R. Dreyer, H.-P. Jia, C.W. Bielawski, Graphene Oxide: A Convenient Carbocatalyst for Facilitating Oxidation and Hydration Reactions, Angew. Chemie. 122 (2010) 6965–6968. https://doi.org/10.1002/ange.201002160.

[5] S. Navalon, A. Dhakshinamoorthy, M. Alvaro, H. Garcia, Carbocatalysis by graphene-based materials, Chem. Rev. 114 (2014) 6179–6212. https://doi.org/10.1021/cr4007347.

[6] X. Duan, H. Sun, S. Wang, Metal-Free Carbocatalysis in Advanced Oxidation Reactions, Acc. Chem. Res. 51 (2018) 678–687. https://doi.org/10.1021/acs.accounts.7b00535.

[7] X. Duan, Z. Ao, H. Sun, S. Indrawirawan, Y. Wang, J. Kang, F. Liang, Z.H. Zhu, S. Wang, Nitrogen-doped graphene for generation and evolution of reactive radicals by metal-free catalysis, ACS Appl. Mater. Interfaces. 7 (2015) 4169–4178. https://doi.org/10.1021/am508416n.

[8] S. Indrawirawan, H. Sun, X. Duan, S. Wang, Low temperature combustion synthesis of nitrogen-doped graphene for metal-free catalytic oxidation, J. Mater. Chem. A. 3 (2015) 3432–3440. https://doi.org/10.1039/c4ta05940a.

[9] X. Wang, Y. Qin, L. Zhu, H. Tang, Nitrogen-doped reduced graphene oxide as a bifunctional material for removing bisphenols: Synergistic effect between adsorption and catalysis, Environ. Sci. Technol. 49 (2015) 6855–6864. https://doi.org/10.1021/acs.est.5b01059.

[10] X. Chen, T.T. Lim, Highly-efficient peroxymonosulfate activation for sulfacetamide degradation over nitrogen-functionalized graphene: The effect of thermal annealing temperature on reactive functional groups, Chem. Eng. Trans. 73 (2019) 145–150. https://doi.org/10.3303/CET1973025.

[11] H. Chen, K.C. Carroll, Metal-free catalysis of persulfate activation and organic-pollutant degradation by nitrogen-doped graphene and aminated graphene, Environ. Pollut. 215 (2016) 96–102. https://doi.org/10.1016/j.envpol.2016.04.088.

[12] D. Li, X. Duan, H. Sun, J. Kang, H. Zhang, M.O. Tade, S. Wang, Facile synthesis of nitrogen-doped graphene via low-temperature pyrolysis: The effects of precursors and annealing ambience on metal-free catalytic oxidation, Carbon N. Y. 115 (2017) 649–658. https://doi.org/10.1016/j.carbon.2017.01.058.

[13] J. Kang, L. Zhou, X. Duan, H. Sun, S. Wang, Catalytic degradation of antibiotics by metal-free catalysis over nitrogen-doped graphene, Catal. Today. (2018) 0–1. https://doi.org/10.1016/j.cattod.2018.12.002.

[14] X. Chen, W. Da Oh, Z.T. Hu, Y.M. Sun, R.D. Webster, S.Z. Li, T.T. Lim, Enhancing sulfacetamide degradation by peroxymonosulfate activation with N-doped graphene produced through delicately-controlled nitrogen functionalization via tweaking thermal annealing processes, Appl. Catal. B Environ. 225 (2018) 243–257. https://doi.org/10.1016/j.apcatb.2017.11.071.

[15] P. Sun, H. Liu, Z. Zhai, X. Zhang, Y. Fang, J. Tan, J. Wu, Degradation of UV filter BP-1 with nitrogen-doped industrial graphene as a metal-free catalyst of peroxymonosulfate activation, Chem. Eng. J. 356 (2019) 262–271. https://doi.org/10.1016/j.cej.2018.09.023.

[16] J. Kang, X. Duan, L. Zhou, H. Sun, M.O. Tadé, S. Wang, Carbocatalytic activation of persulfate for removal of antibiotics in water solutions, Chem. Eng. J. 288 (2016) 399–405. https://doi.org/10.1016/j.cej.2015.12.040.

[17] Q. Wang, L. Li, L. Luo, Y. Yang, Z. Yang, H. Li, Y. Zhou, Activation of persulfate with dual-doped reduced graphene oxide for degradation of alkylphenols, Chem. Eng. J. 376 (2019) 120891. https://doi.org/10.1016/j.cej.2019.01.170.

[18] X. Duan, K. O'Donnell, H. Sun, Y. Wang, S. Wang, Sulfur and Nitrogen Co-Doped Graphene for Metal-Free Catalytic Oxidation Reactions, Small. 11 (2015) 3036–3044. https://doi.org/10.1002/smll.201403715.

[19] P. Sun, H. Liu, M. Feng, L. Guo, Z. Zhai, Y. Fang, X. Zhang, V.K. Sharma, Nitrogen-sulfur co-doped industrial graphene as an efficient peroxymonosulfate activator: Singlet oxygen-dominated catalytic degradation of organic contaminants, Appl. Catal. B Environ. 251 (2019) 335–345. https://doi.org/10.1016/j.apcatb.2019.03.085.

[20] H. Sun, Y. Wang, S. Liu, L. Ge, L. Wang, Z. Zhu, S. Wang, Facile synthesis of nitrogen doped reduced graphene oxide as a superior metal-free catalyst for oxidation, Chem. Commun. 49 (2013) 9914–9916. https://doi.org/10.1039/c3cc43401j.

[21] H. Sun, S. Liu, G. Zhou, H.M. Ang, M.O. Tadé, S. Wang, Reduced graphene oxide for catalytic oxidation of aqueous organic pollutants, ACS Appl. Mater. Interfaces. 4 (2012) 5466–5471. https://doi.org/10.1021/am301372d.

[22] X. Duan, H. Sun, J. Kang, Y. Wang, S. Indrawirawan, S. Wang, Insights into

795 Heterogeneous Catalysis of Persulfate Activation on Dimensional-Structured
796 Nanocarbons, ACS Catal. 5 (2015) 4629–4636.
797 https://doi.org/10.1021/acscatal.5b00774.
798 [23] T. Olmez-Hanci, I. Arslan-Alaton, S. Gurmen, I. Gafarli, S. Khoei, S. Safaltin, D.
799 Yesiltepe Ozcelik, Oxidative degradation of Bisphenol A by carbocatalytic
800 activation of persulfate and peroxymonosulfate with reduced graphene oxide, J.
801 Hazard. Mater. 360 (2018) 141–149.
802 https://doi.org/10.1016/j.jhazmat.2018.07.098.
803 [24] S. Wang, J. Wang, Kinetics of PMS activation by graphene oxide and biochar,
804 Chemosphere. 239 (2020) 124812.
805 https://doi.org/10.1016/j.chemosphere.2019.124812.
806 [25] R.R. Solís, I.F. Mena, M.N. Nadagouda, D.D. Dionysiou, Adsorptive interaction
807 of peroxymonosulfate with graphene and catalytic assessment via non-radical
808 pathway for the removal of aqueous pharmaceuticals, J. Hazard. Mater. 384 (2020)
809 121340. https://doi.org/10.1016/j.jhazmat.2019.121340.
810 [26] Y. Liu, L. Yu, C.N. Ong, J. Xie, Nitrogen-doped graphene nanosheets as reactive
811 water purification membranes, Nano Res. 9 (2016) 1983–1993.
812 https://doi.org/10.1007/s12274-016-1089-7.
813 [27] M. Pedrosa, G. Drazic, P.B. Tavares, J.L. Figueiredo, A.M.T. Silva, Metal-free
814 graphene-based catalytic membrane for degradation of organic contaminants by
815 persulfate activation, Chem. Eng. J. 369 (2019) 223–232.
816 https://doi.org/10.1016/j.cej.2019.02.211.
817 [28] O. Vieira, R.S. Ribeiro, M. Pedrosa, A.R. Lado Ribeiro, A.M.T. Silva, Nitrogen-
818 doped reduced graphene oxide – PVDF nanocomposite membrane for persulfate
819 activation and degradation of water organic micropollutants, Chem. Eng. J. 402
820 (2020) 126117. https://doi.org/10.1016/j.cej.2020.126117.
821 [29] J. Sheng, H. Yin, F. Qian, H. Huang, S. Gao, J. Wang, Reduced graphene oxide-
822 based composite membranes for in-situ catalytic oxidation of sulfamethoxazole
823 operated in membrane filtration, Sep. Purif. Technol. 236 (2020) 116275.
824 https://doi.org/10.1016/j.seppur.2019.116275.
825 [30] Y. Wang, Z. Ao, H. Sun, X. Duan, S. Wang, Activation of peroxymonosulfate by
826 carbonaceous oxygen groups: Experimental and density functional theory
827 calculations, Appl. Catal. B Environ. 198 (2016) 295–302.
828 https://doi.org/10.1016/j.apcatb.2016.05.075.

[31] X. Duan, H. Sun, Z. Ao, L. Zhou, G. Wang, S. Wang, Unveiling the active sites of graphene-catalyzed peroxymonosulfate activation, Carbon N. Y. 107 (2016) 371–378. https://doi.org/10.1016/j.carbon.2016.06.016.

[32] X. Duan, Z. Ao, L. Zhou, H. Sun, G. Wang, S. Wang, Occurrence of radical and nonradical pathways from carbocatalysts for aqueous and nonaqueous catalytic oxidation, Appl. Catal. B Environ. 188 (2016) 98–105. https://doi.org/10.1016/j.apcatb.2016.01.059.

[33] L. Sbardella, I.V. Gala, J. Comas, S.M. Carbonell, I. Rodríguez-Roda, W. Gernjak, Integrated assessment of sulfate-based AOPs for pharmaceutical active compound removal from wastewater, J. Clean. Prod. 260 (2020) 121014. https://doi.org/10.1016/j.jclepro.2020.121014.

[34] R.S. Ribeiro, Z. Frontistis, D. Mantzavinos, D. Venieri, M. Antonopoulou, I. Konstantinou, A.M.T. Silva, J.L. Faria, H.T. Gomes, Magnetic carbon xerogels for the catalytic wet peroxide oxidation of sulfamethoxazole in environmentally relevant water matrices, Appl. Catal. B Environ. 199 (2016) 170–186. https://doi.org/10.1016/j.apcatb.2016.06.021.

[35] Modification of the surface chemistry of activated carbons, Carbon N. Y. 37 (n.d.) 1379–1389. https://doi.org/10.1016/S0008-6223(98)00333-9.

[36] J.L. Figueiredo, M.F.R. Pereira, M.M.A. Freitas, J.J.M. Órfão, Characterization of active sites on carbon catalysts, Ind. Eng. Chem. Res. 46 (2007) 4110–4115. https://doi.org/10.1021/ie061071v.

[37] A. Bianco, H.M. Cheng, T. Enoki, Y. Gogotsi, R.H. Hurt, N. Koratkar, T. Kyotani, M. Monthioux, C.R. Park, J.M.D. Tascon, J. Zhang, All in the graphene family - A recommended nomenclature for two-dimensional carbon materials, Carbon N. Y. 65 (2013) 1–6. https://doi.org/10.1016/j.carbon.2013.08.038.

[38] G. V Buxton, C.L. Greenstock, W.P. Helman, A.B. Ross, Critical Review of rate constants for reactions of hydrated electrons, hydrogen atoms and hydroxyl radicals in aqueous solution, J. Phys. Chem. Ref. Data. 17 (1988) 513. https://doi.org/10.1063/1.555805.

[39] R.E. Huie, P. Neta, A.B. Ross, Rate Constants for Reactions of Inorganic Radicals in Aqueous Solution, J. Phys. Chem. Ref. Data. 17 (1988). https://doi.org/10.1063/1.555978.

[40] F. Wilkinson, J.G. Brummer, Rate constants for the decay and reactions of the lowest electronically excited singlet state of molecular oxygen in solution, J. Phys.

Chem. Ref. Data. 10 (1981) 809–999. https://doi.org/10.1063/1.555655.

[41] E. Fuente, J.A. Menéndez, D. Suárez, M.A. Montes-Morán, Basic surface oxides on carbon materials: A global view, Langmuir. 19 (2003) 3505–3511. https://doi.org/10.1021/la026778a.

[42] Y. Zhou, J. Jiang, Y. Gao, J. Ma, S.Y. Pang, J. Li, X.T. Lu, L.P. Yuan, Activation of Peroxymonosulfate by Benzoquinone: A Novel Nonradical Oxidation Process, Environ. Sci. Technol. 49 (2015) 12941–12950. https://doi.org/10.1021/acs.est.5b03595.

[43] X. Cheng, H. Guo, Y. Zhang, X. Wu, Y. Liu, Non-photochemical production of singlet oxygen via activation of persulfate by carbon nanotubes, Water Res. 113 (2017) 80–88. https://doi.org/10.1016/j.watres.2017.02.016.